Inorganic Chemistry

Article

pubs.acs.org/IC

Molybdenum(VI) Dioxo and Oxo-Imido Complexes of Fluorinated β-Ketiminato Ligands and Their Use in OAT Reactions

Manuel Volpe and Nadia C. Mösch-Zanetti*

Institut für Chemie, Bereich Anorganische Chemie, Karl-Franzens-Universität, Graz Stremayrgasse 16, A-8010 Graz, Austria

Supporting Information

ABSTRACT: Substitution of a methyl by a trifluoromethyl moiety in well-known β-ketimines afforded the ligands (Ar)NC(Me)CH_2CO(CF_3) (HL^H, Ar = C_6H_5; HL^{Me}, A r= 2,6-$Me_2C_6H_3$; HL^{iPr}, Ar = 2,6-$^iPr_2C_6H_3$). Subsequent complexation to the $[MoO_2]^{2+}$ core leads to the formation of novel complexes of general formula $[MoO_2(L^R)_2]$ (R = H, **1**; R = Me, **2**; R = iPr, **3**). For reasons of comparison the oxo-imido complex $[MoO(N^tBu)(L^{Me})_2]$ (**4**) has also been synthesized. Complexes **1**−**4** were investigated in oxygen atom transfer (OAT) reactions using the substrate trimethylphosphine. The respective products after OAT, the reduced Mo^{IV} complexes $[MoO(PMe_3)(L^R)_2]$ (R = H, **5**; R = Me, **6**; R = iPr, **7**) and $[Mo(N^tBu)(PMe_3)(L^{Me})_2]$ (**8**), were isolated. All complexes have been characterized by NMR spectroscopy, and **1**−**4** also by cyclic voltammetry. A positive shift of the Mo^{VI}−Mo^V reduction wave upon fluorination was observed. Furthermore, molecular structures of complexes **2**, **4**, **5**, and **8** have been determined via single crystal X-ray diffraction analysis. Complex **8** represents a rare example of a Mo^{IV} phosphino-imido complex. Kinetic measurements by UV−vis spectroscopy of the OAT reactions from complexes **1**−**4** to PMe_3 showed them to be more efficient than previously reported nonfluorinated ones, with ligand L′ = (Ar)NC(Me)CH_2CO(CH_3) $[MoO_2(L')_2]$ (**9**) and $[MoO(N^tBu)(L')_2]$ (**10**), respectively. Thermodynamic activation parameters $\Delta H^{\ddagger}$ and $\Delta S^{\ddagger}$ of the OAT reactions for complexes **2** and **4** have been determined. The activation enthalpy for the reaction employing **2** is significantly smaller (12.3 kJ/mol) compared to the reaction with the nonfluorinated complex **9** (60.8 kJ/mol). The change of the entropic term $\Delta S^{\ddagger}$ is small. The reaction of the oxo-imido complex **4** to **8** revealed a significant electron-donating contribution of the imido substituent.

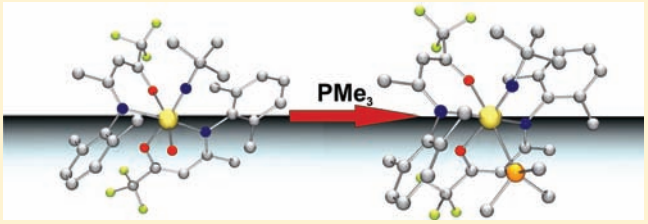

INTRODUCTION

Oxygen atom transfer (OAT) belongs to the fundamental reactions that have both industrial and biological relevance: in industry, it is used to afford epoxides from readily available olefins,[1] while living organisms utilize OAT in metabolic processes such as the degradation of xanthine to uric acid.[2−4] Both processes are mediated by molybdenum. Synthetic catalysts are often molybdenum dioxo complexes due the readily availability of the $[MoO_2Cl_2]$ starting material.[5] In biological systems, OAT is catalyzed by various molybdoenzymes which modulate the reactivity on the basis of the structure of their active centers: according to this, these enzymes can be classified into three different families, xanthine oxidase, sulfite oxidase, and DMSO reductase families. The structures of several of these enzymes have been characterized by X-ray crystallography.[3,6−10] In all cases the mononuclear molybdenum center is coordinated by at least one terminal oxo group and by one or two pterin based ligands. Furthermore, depending on the family a second oxo group (sulfite oxidase), a sulfido group (xanthine oxidase), or a nondoubly bonded group (DMSO reductase) is found in the active site. Due to this structural diversity, function−structure relationships are complex and as yet not fully understood. For this reason, much biomimetic chemistry has been devoted to this class of enzymes.[5,11,12]

For a better understanding of mechanistic aspects of OAT reactions in general, we developed Schiff-base Mo(VI) complexes $[MoO(X)(L)_2]$ (X = O, N^tBu; L = bidentate Schiff base ligands) and investigated their reactivity in OAT.[13] The imido functionality was introduced in an attempt to simulate the presence of a second doubly bonded nonoxygen atom as found in xanthine oxidase. Although an imido group is not a close substitute for a sulfide group, its introduction allows the differentiation of the doubly bonded moieties at molybdenum. In addition, oxo-sulfido species are significantly more challenging to prepare, no convenient starting materials are available, and they usually display a high tendency for dimerization under formation of a disulfide bridge $[(L)_2OMoS{-}SMoO(L)_2]$. Rare examples showed that high steric demand works against it allowing the isolation of [(Tp)MOS(OAr)] (Tp = tris(pyrazolyl)borate).[14,15] Although the imido ligand is not found in the active sites of the enzyme families, such compounds represent examples of monooxo molybdenum(VI) compounds related to xanthine oxidase and DMSO reductase, which are limited in the literature.[16−19] We found them to be stable toward dimerization, presumably due to the steric demand at the tert-butyl imido nitrogen, and to be

Received: August 3, 2011
Published: January 23, 2012

dx.doi.org/10.1021/ic201681u | Inorg. Chem. 2012, 51, 1440−1449

active in the OAT reaction to trimethyl phosphine. Comparison of the oxo-imido to corresponding dioxo compounds allowed us to investigate the influence of the second doubly bonded ligand at molybdenum. The oxygen atom transfer is influenced by the imido and the β-ketiminato ligand with a fine interplay of steric and electronic effects.[13] However, we observed a small influence of various aromatic substitutents at the nitrogen donor of the ketiminato ligand. Variation of the substituent at the imido nitrogen would be desirable, but other than with the N^{t}Bu group, molybdenum oxo-imido compounds are synthetically challenging.[20−24] Only recently a synthetic procedure for the N^{t}Bu imido precursor has been reported from which some coordination chemistry was developed.[25−30] Therefore, we decided to investigate ligand backbone substitution and introduced a CF_3 functionality (Figure 1) which removes electronic density at the metal center

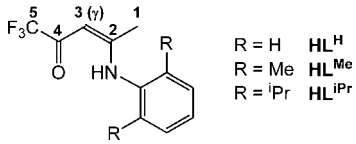

Figure 1. General scheme of ligands presented in this work.

and should make the electron donation capability of the imido group more pronounced.[31]

The aniline derived trifluoromethyl substituted ligand HL^H (phenylimino-1,1,1-trifluoropentan-2-one) employed in this study has been known for some time,[32] whereas the methyl and iso-propyl substituted versions have just very recently been published. They were mainly used as ancillary ligands in group 4 and 5 complexes suitable for ethylene polymerizations.[33−36] Furthermore, norbornene and ^{t}Bu-metacrylate have been coupled in the presence of a Ni^{II} derivative of such Schiff bases,[37,38] and the literature reports a single example of a half-sandwich Cr^{III} complex, also an olefin polymerization catalyst.[39] Incorporation of this fluorinated β-ketiminato motive in a more elaborated, macrocyclic framework has also been reported for VO^{2+} and Cu^{II} complexes.[40] In all of the reported cases, catalyst performance has been improved. No molybdenum complexes containing the fluorinated HL^R ligands (R = H, Me, ^{i}Pr) were known before the present work.

This work describes the preparation of dioxo $[MoO_2(L^R)_2]$ (**1**−**3**) and the oxo-imido Mo(VI) $[MoO(N^tBu)(L^{Me})_2]$ (**4**) complexes with 2,6-disubstituted phenylimino-1,1,1-trifluoropentan-2-ones HL^R (R = H, Me, iPr), the isolation of reduced compounds $[MoO(PMe_3)(L^R)_2]$ (**5**−**7**) and $[Mo(N^tBu)(PMe_3)(L^{Me})_2]$ (**8**), as well as a comparison to the previously published nonfluorinated analogues $[MoO_2(L')_2]$ (**9**)[42] and $[MoO(N^tBu)(L')_2]$ (**10**) (Figure 2).[13] Kinetic investigations provide an interesting insight into the influence of electronic factors on the rate of the OAT reaction.

RESULTS AND DISCUSSION

Ligand Synthesis. Ligands (Ar)NC(Me)$CH_2CO(CF_3)$ (HL^H, Ar = C_6H_5; HL^{Me}, Ar = 2,6-$Me_2C_6H_3$; HL^{iPr}, Ar = 2,6-$^i Pr_2C_6H_3$) employed in this study have been synthesized by a modified literature procedure by Schiff base condensation of 1,1,1-trifluoropentane-2,4-dione with the respective anilines.[32−36] We have found that azeotropic removal of water is not necessary and the syntheses can be carried out in an one-pot reaction in benzene with molecular sieves. In this way, much higher yields up to 70% can be achieved in 3 h reaction

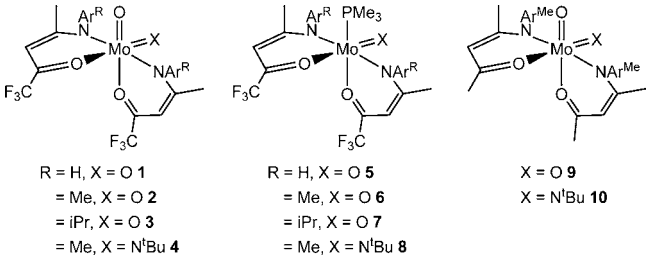

Figure 2. Numbering scheme of the here described complexes **1**−**8** and the previously published **9** and **10**.

time. In principle, there are two possible regioisomers (Figure 3). Following our procedure, the reaction affords purely the CF_3CO

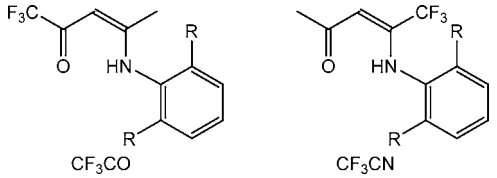

Figure 3. Possible isomers with respect to the position of CF_3.

isomer, whereas when more polar solvents are used, both isomers CF_3CO and CF_3CN are observed, especially in the case of HL^H.[41]

Preparation of Molybdenum(VI) Complexes. The complexes $[MoO_2(L^R)_2]$ (R = H, **1**; R = Me, **2**; R = iPr, **3**) can be synthesized from $[MoO_2Cl_2]$ by addition of the respective ligand and NEt_3 in toluene. All compounds were obtained as yellow to orange crystalline solids by recrystallization from pentane/toluene. They are well soluble in polar solvents such as THF or MeCN as well as in toluene, but insoluble in aliphatic solvents.

$$[MoO_2Cl_2] + 2HL^R \xrightarrow[-2NEt_3HCl]{+2NEt_3} [MoO_2(L^R)_2]$$

$$R = H,\ \mathbf{1}$$
$$= Me,\ \mathbf{2}$$
$$= {}^iPr,\ \mathbf{3} \qquad (1)$$

NMR spectroscopy displayed for complexes **1**−**3** one set of ligand resonances indicating single isomers in solution (i.e., no *cis*−*trans* N,N or N,O distribution is observed).[42] Particularly indicative in this regard are the ^{1}H NMR spectra in the region at around 5 ppm, where only a single signal, assignable to the γ-H in the ligand backbone ($\Delta\delta$ = 0.2−0.3 ppm downfield with respect to the free ligand), can be seen. Only one singlet in this region points to a symmetric coordination mode around the metal center. Further confirmation is given by the ^{19}F NMR spectra, which show one resonance for the two equivalent CF_3 groups quite distinct from the free ligand ($\Delta\delta \approx 2$ ppm).

In order to vary not only the sterics around the Mo center, but also the electronics, one representative oxo-imido complex $[MoO(N^tBu)(L^{Me})2]$ (**4**) was prepared. Its synthesis was carried out from the chloro precursor $[MoO(N^tBu)Cl_2(dme)]$ and HL^{Me} affording the product as a single isomer (eq 2). The compound is obtained in moderate yield as a yellow powder, is extremely sensitive to hydrolysis, and is readily soluble in most common organic solvents.

Quite obviously, in this case the equivalency of the γ-H and CF_3 resonances is lost, the former appearing as two signals at 5.63 and 5.53 ppm in the ^{1}H NMR spectrum and the latter as a

dx.doi.org/10.1021/ic201681u | Inorg. Chem. 2012, 51, 1440−1449

pair of singlets at −73.24 and −72.36 ppm in the ^{19}F NMR spectrum, respectively.

$$[MoO(N^tBu)Cl_2(dme)] + 2HL^{Me} \xrightarrow[-2NEt_3HCl]{+NEt_3} [MoO(N^tBu)(L^{Me})_2] \quad (2)$$
$$\xrightarrow[-dme]{} \mathbf{4}$$

During an attempted crystallization of **1**, a single crystal of the mixed oxo anilido derivative $[MoO(N(2,6\text{-}Me_2C_6H_3))(L^{Me})_2]$ could be picked out of the vessel (Figure S1 and Table S1 in Supporting Information). The formation of this quite unusual derivative is probably due to adventitious traces of water which hydrolyzed the Schiff base ligand, decomposing it into its aniline component, which then proceeded to react with a Mo═O moiety. Although a rational synthesis of $[MoO(NR)]^{2+}$ compounds with various R groups would be highly desirable,[20−22,24] several attempts to synthesize this compound in a rational way (i.e., reaction with 2,6-dimethylaniline, a respective isocyanate,[43,44] or sulfinylamine)[45] have not been successful.

Oxygen Atom Transfer Reactivity. Complexes **1**−**3** undergo OAT reaction to PMe_3 affording the corresponding Mo(IV) monooxo derivatives **5**−**7** according to eq 3, with elimination of 1 equiv of $OPMe_3$.

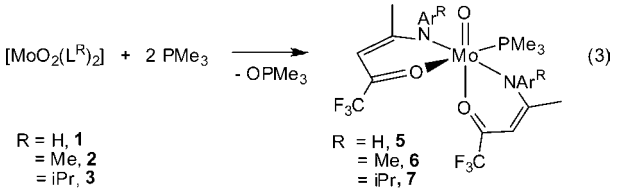

The reaction color changes quickly from orange to green upon addition of the phosphine. After removal of the solvent and subsequent removal of the $OPMe_3$ byproduct by sublimation (0.05 mmHg, 70 °C) deep green powders were obtained. They are very soluble in aromatic and polar solvents. The ^1H NMR spectra of derivatives **5**−**7** in benzene-d_6 show two sets of resonances for the coordinated ligands as expected for the change of chemical environment upon PMe_3 coordination for the two ketiminato ligands. Furthermore, the spectra exhibit a high-field doublet ($\delta \approx 0.5$ ppm), which integrates for 9 protons, consistent with a coordinated PMe_3 ligand. Coordination of the phosphorus ligand is also evident in the ^{31}P NMR spectra of the complexes, where a single signal, intermediate in position between those of PMe_3 and $OPMe_3$ ($\delta = -1.28$ ppm (**5**), $\delta = -7.10$ ppm (**6**), $\delta = -1.24$ ppm (**7**)), can be detected. Mass spectrometry, even when very mild ionization techniques are used, fails to provide the correct molecular peak, the highest mass corresponding instead to the $[MoO(L)_2]$ fragment.

The OAT reaction between the oxo-imido derivative **4** and PMe_3 leads to reduced complex **8** as shown in eq 4.

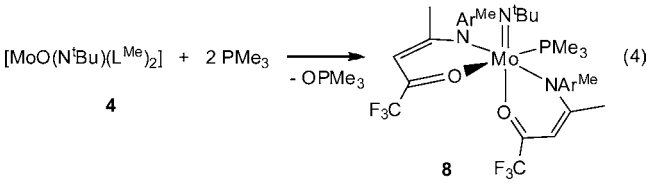

A solution of the yellow complex **4** turns very rapidly to purple upon addition of 2 equiv of PMe_3. After workup and removal of the phosphine oxide by sublimation, compound $[Mo(N^tBu)(PMe_3)(L^{Me})_2]$ (**8**) can be recovered as a violet powder which is moderately soluble in aromatic solvents and THF and completely insoluble in aliphatic ones. The ^1H NMR and ^{19}F NMR spectra of **8**, again, point to the existence of a single isomer in solution. The ^{31}P NMR spectrum shows a single signal at 2.82 ppm for the coordinated phosphine, whose protons can be observed as a doublet at 0.51 ppm in the ^1H NMR spectrum.

Experiments to investigate the kinetics of OAT reactions of **1**−**4** by UV−vis spectroscopy were investigated under pseudo-first-order conditions in PMe_3. All reactions were performed in toluene at 20 °C with a defined excess of PMe_3 (50−150 equiv of phosphine). The reaction progress was monitored by the appearance of a peak in the visible region of the electronic spectrum (**1**−**3** λ_{max} = 480 nm, **4** λ_{max} = 517 nm). These absorptions are identical to those found in the isolated compounds **5**−**8**. As a representative example, UV−vis data is shown for the reduction of **2** at different PMe_3 concentrations allowing the determination of the second-order rate constant. For UV−vis data on complex **4**, see Supporting Information. The individual rate constants k_{obs} were obtained by fitting the data to a first-order rate law. Clean transformation from the Mo^{VI} to Mo^{IV} species was confirmed throughout the kinetic experiments by the appearance of an isosbestic point. Second-order rate constants k_2 were deducted from the linear plot at the various PMe_3 concentrations (Figure 4).

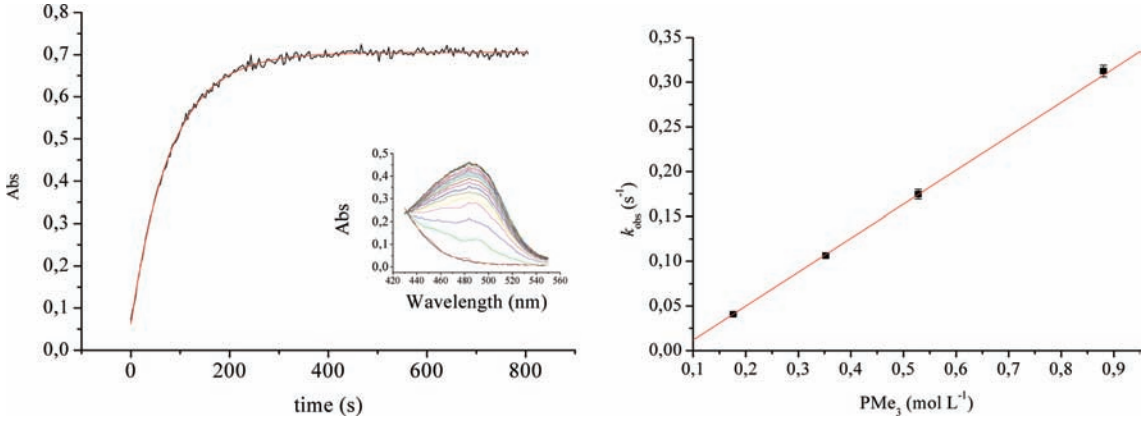

Figure 4. Left: UV−vis spectroscopy at 480 nm of the reaction of **2** with 150 equiv of PMe_3, superimposed with a nonlinear fit of the data. In the inset, plot of the actual spectra (Δt = 10 s). Right: determination of the second-order rate constant.

dx.doi.org/10.1021/ic201681u | Inorg. Chem. 2012, 51, 1440−1449

The results for the determination of the second-order rate constants of complexes **1**−**4** are summarized in Table 1. In the case of **1**, the reaction is completed in a few seconds (in this case a full spectrum per measurement could not be acquired and the reaction was monitored at a single wavelength).

Table 1. Second-Order Rate Constants k_2 for the OAT Reaction for 1−4

complex	k_2 (M^{-1} s^{-1})
$[MoO_2(L^H)_2]$ (**1**)	9(1)
$[MoO_2(L^{Me})_2]$ (**2**)	$3.79(5) \times 10^{-1}$
$[MoO_2(L^{iPr})_2]$ (**3**)	$2.56(3) \times 10^{-3}$
$[MoO(N^tBu)(L^{Me})_2]$ (**4**)	$2.76(1) \times 10^{-2}$

The reaction rate in going from the unsubstituted derivative **1** to the ^{i}Pr one (**3**) decreases which can be explained with an increase in the steric protection around the oxo moieties, as already experienced in the series of nonfluorinated derivatives. A general increase in the OAT reaction rate is observed compared to the nonfluorinated corresponding derivatives: for complex **2**, the increase is 92-fold ($4.1(2) \times 10^{-3}$ M^{-1} s^{-1} for **9**, Table 2).[42] The second-order rate constant which has been found for derivative **4**, $2.76(1) \times 10^{-2}$ M^{-1} s^{-1}, is 15 times bigger than the corresponding value for the methylated derivative ($1.83(1) \times 10^{-3}$ M^{-1} s^{-1}, Table 2).[13] The rate increase of the oxo-imido complex **4** versus **10** is not as evident as in the dioxo case. The importance of the CF_3 contribution can also be observed in the fact that, whereas **3** reacts with PMe_3, albeit slowly, no reaction at all is observed when the CF_3 group is substituted by a CH_3.[42] This supports the mechanistic idea of a nucleophilic attack of the incoming phosphine onto the oxo atom of the complex: the CF_3 groups act as electron sinks for the complex, thus leaving the oxo atoms more susceptible to nucleophilic attacks.

Table 2. Second-Order Rate Constants k_2 for the Fluorinated and Nonfluorinated Derivatives (M^{-1} s^{-1}) Showing the Ratio of Rate Increase

	CF_3 derivative	CH_3 derivative	ratio $k_2(CF_3)/k_2(CH_3)$
$[MoO_2(L^{Me})_2]$: **2** vs **9**	$3.79(5) \times 10^{-1}$	$4.1(2) \times 10^{-3}$	92
$[MoO(N^tBu)(L^{Me})_2]$: **4** vs **10**	$2.76(1) \times 10^{-2}$	$1.83(1) \times 10^{-3}$	15
ratio k_2(dioxo)/k_2(oxo-imido)	14	2	

Experiments in which a CF_3 moiety was inserted in the complex periphery to examine the influence of the electron withdrawing effect have also been recently published by Basu et al. on a tris(pyrazolyl)borate Mo phenolate complex.[46] In this case a 2-fold increase in the reaction rate was observed in going from the H to CF_3 substituted ligand, in contrast to our 92-fold increase, consistent with the shorter distance of the CF_3 group from the metal oxo core.

Furthermore, we determined the thermodynamic activation parameters $\Delta H^{\ddagger}$ and $\Delta S^{\ddagger}$ for complex **2** and compared them to those of the nonfluorinated **9** by running kinetic experiments at different temperatures ($k_2 = 3.79(5) \times 10^{-1}$ at 293.15 K; $k_2 = 4.74(6) \times 10^{-1}$ at 303.15 K and $k_2 = 5.62(1) \times 10^{-1}$ at 313.15 K). In the present case, the activation enthalpy $\Delta H^{\ddagger}$ amounts to 12.3(6) kJ/mol, a significant decrease when compared to the value for corresponding nonfluorinated derivative (60.8 kJ/mol for **9**).[42] The activation enthropy $\Delta S^{\ddagger}$, on the other hand, lies still in the same negative range (−208 vs −112 J/mol) as expected for an associative process.

A summary of all reaction rates is given in Table 2. The 92-fold increase in reaction rate between **2** and **9** versus the 15-fold increase in the oxo-imido complexes (**4** to **10**) is interesting. As the change in sterics going from the CF_3 to the CH_3 derivatives is identical in both systems (dioxo and oxo-imido), the significantly smaller increase of the rate ratio in the case of the oxo-imido complexes can most likely be attributed to the electron-donating capacity of the imido group. The steric demand of the imido group decreases the overall rate of OAT. However, in the absence of an electronic effect of the imido group we would also expect an increase of the rate ratio of approximately 100 in the oxo-imido compounds going from the CH_3 to the CF_3 derivative. The fact that an increase of only 15 is observed can thus be attributed to a significant electron-donation. Similarly, this is evidenced by comparison of the two dioxo/oxo-imido couples in the CF_3 and CH_3 case (Table 2). The difference in increase of the ratio in the CF_3 derivatives is with 14 much higher than the 2-fold increase in the CH_3 case. Electron donation of the imido group in the electron depleted system decreases the rate much more profoundly.

Electrochemical Investigations. To further probe the influence of the backbone fluorination, cyclic voltammetry experiments were performed on all of the three derivatives, and the results are displayed in Figure 5.

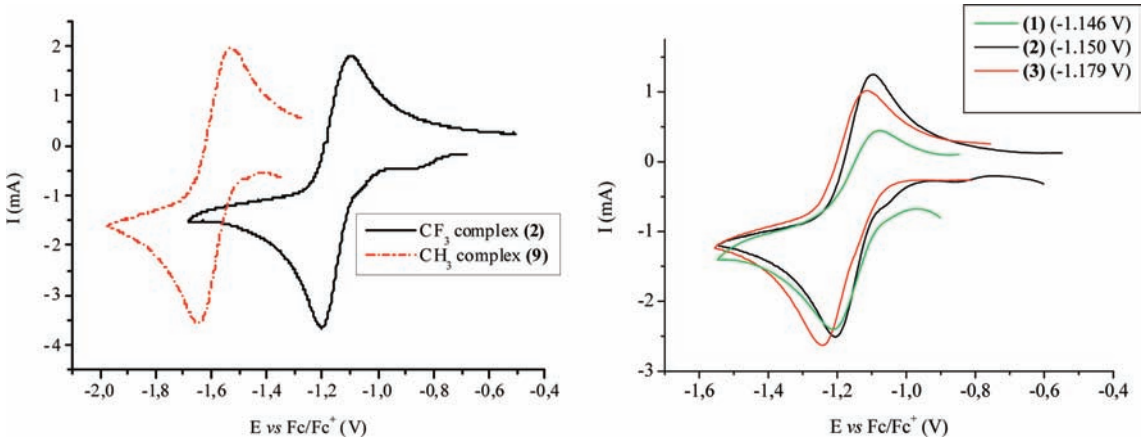

Figure 5. Left: comparison of cyclic voltammograms of $[MoO_2(L^{Me})_2]$ (**2**) (solid line) and nonfluorinated analogue **9** (dotted line). Right: comparison of cyclic voltammograms of the dioxo derivatives **1**−**3**. Conditions: MeCN, $[NBu_4][PF_6]$ (0.2 M), 100 mV s^{-1}, vs Fc/Fc^+, only the molybdenum couple is shown. Full voltammogram is shown in Figure S3.

dx.doi.org/10.1021/ic201681u | Inorg. Chem. 2012, 51, 1440−1449

Upon fluorination of the ligand backbone, all of the dioxo complexes show a single reversible wave assignable to the Mo(VI)/Mo(V) couple, sensibly shifted to less negative potentials with respect to the methyl substituted analogue (e.g., −1.179 for **2** vs −1.590 V for **9**) supporting once more the notion of facilitated nucleophilic attack. On the other hand, the degree of alkylation of the arene rings does not influence the reduction potential at all: the three derivatives exhibit virtually the same voltammetric behavior. No *+I* inductive effect contribution seems to be operating in these systems. This renders the substitution by a CF_3 group described in this work even more important for the investigation of the electronic effects.

Such a behavior is also observed in the cyclic voltammetry trace of **4** in MeCN (Figure 6): the oxo-imido derivative shows

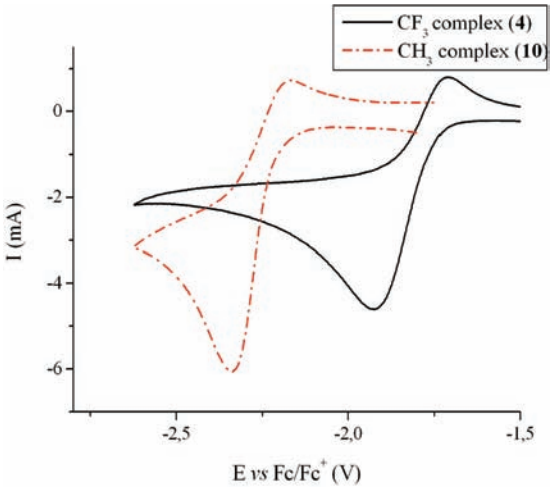

Figure 6. Comparison of cyclic voltammetram of $[MoO(N^tBu)(L^{Me})_2]$ (**4**) and the nonfluorinated analogue **10**. Conditions: MeCN, $[NBu_4][PF_6]$ (0.2 M), 100 mV s^{-1}, vs Fc/Fc^+. Only the molybdenum couple is shown.

a quasireversible redox wave at −1.83 V, similar in shape to the one exhibited by the corresponding nonfluorinated compound **10**.

Molecular Structures of the Compounds. Complex **2**, **4**, **5**, and **8** were subjected to a single crystal X-ray diffraction study (Figure 7).

Complex **2** crystallized from a cold (−30 °C) saturated MeCN solution in the form of small orange blocks, while crystals of **4** could be obtained by vapor diffusion of pentane in a THF solution of the complex as small yellow blocks. Selected bond distances and angles are reported in Table 3 and crystallographic data in Table 5.

Table 3. Selected Bond Distances (Å) and Angles (deg) for $[MoO_2(L^{Me})_2]$ (2) and $[MoO(N^tBu)(L^{Me})_2]$ (4)

	$[MoO_2(L^{Me})_2]$ (**2**)	$[MoO(NtBu)(L^{Me})_2]$ (**4**)
Mo1−O1	1.7150(12)	1.7131(12)
Mo1−O2	1.7050(11)	
Mo1−N3		1.7411(15)
Mo1−N1	2.1578(12)	2.1798(13)
Mo1−N2	2.1792(13)	2.1965(13)
Mo1−O3	2.1374(11)	2.1458(12)
Mo1−O4	2.1028(11)	2.1646(13)
Mo1−N3−C27		175.92(13)
O1−Mo1−E (E = O2, N3)	103.88(6)	104.31(7)
O2−Mo1−O3	166.47(5)	
O2−Mo1−N3		166.44(3)

Both compounds display the same *trans*-N,N arrangement of the bidentate *β*-ketiminato ligands, with the oxo or the ^{t}Bu-imido groups completing the octahedral coordination sphere around the molybdenum atom. In the case of **4**, the N^tBu group coordinates essentially linearly to the metal atom (the Mo1−N3−C27 angle being 175.9(1)°), as reported for several other Mo^{VI} ^{t}Bu-imido complexes of similar structure. Quite surprisingly, neither the Mo═O or the Mo═N bond distances in both complexes seem to be affected by the electron-withdrawing properties of the introduced CF_3 group (i.e., for the Mo=N^{t}Bu in the nonfluorinated analogue of **4**,[13] the reported value is 1.734(2) Å, while in a salpen analogue[26] it is at 1.739(1) Å). No significant elongation could be similarly found for the C−O moiety of the ligand, more closely bound to the electronegative group.

Complex **5** crystallized from a saturated toluene solution at −30 °C as deep green blocks (which were found to contain a molecule of toluene per molecule of complex) in the

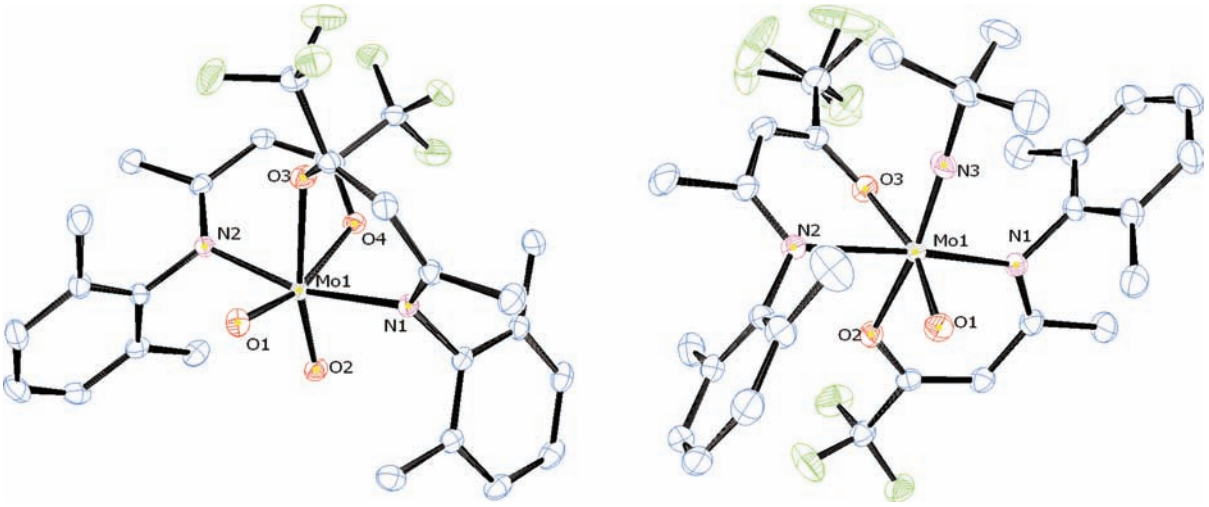

Figure 7. ORTEP drawings of the crystal structures of $[MoO_2(L^{Me})_2]$ (**2**) (right) and $[MoO(N^tBu)(L^{Me})_2]$ (**4**) (left). Thermal ellipsoids are drawn at 30% probability level, and hydrogen atoms are omitted for clarity.

dx.doi.org/10.1021/ic201681u | *Inorg. Chem.* 2012, 51, 1440−1449

monoclinic space group $P2_1/c$. Selected bond lengths and angles are reported in Table 4 and crystallographic data in Table 5. In the structure, the Mo atom sits in a (distorted) octahedral coordination environment constituted by a terminal oxo atom, the two N,O bidentate β-ketiminato ligands and a phosphorus atom of a PMe_3 molecule, similarly to the arrangement found in the nonfluorinated complex $[MoO(PMe_3)L_2]$.[42] Unfortunately, for this previously reported nonfluorinated derivative, the quality of the X-ray diffraction data was not good enough to allow for a meaningful comparison.

Table 4. Selected Bond Distances (Å) and Angles (deg) for $[MoO(PMe_3)(L^H)_2]$ (5) and $[Mo(N^tBu)(PMe_3)(L^{Me})_2]$ (8)

	$[MoO(PMe_3)(L^H)_2]$ (5)	$[Mo(N^tBu)(PMe_3)(L^{Me})_2]$ (8)
Mo1−O1	1.6833(9)	
Mo1−N3		1.703(3)
Mo1−P1	2.5051(4)	2.5408(10)
Mo1−N1	2.1500(10)	2.2363(10)
Mo1−N2	2.2012(9)	2.2403(11)
Mo1−O2	2.1272(9)	
Mo1−O3	2.1067(9)	
Mo1−O1		2.1236(9)
Mo1−O2		2.1224(12)
O1−Mo1−O2	167.76(4)	
O1−Mo1−N3		173.32(12)
O−Mo1−P1	163.99(2)	166.49(3)

The Mo1−O1 bond distance (1.6833(9) Å) is in the normal range for Mo(IV) monooxo complexes,[47] while the Mo1−P1 separation, at 2.5051(4) Å, is a bit longer than that reported for $[MoO(acac)_2(PMe_3)]$ (2.468(2) Å).[48] Comparable values can be found throughout the literature.[49] The two N atoms of the β-ketiminato ligands are *trans* to each other, forming in this way one axis of the coordination octahedron, but the two bond lengths are not equivalent, measuring at 2.2012(9) and 2.1500(10) Å, respectively. At the same time the reverse behavior is observed for the Mo−O bond distances, where Mo1−O3 (2.1067(9) Å) is significantly shorter than the Mo1−O2 one (2.1272(9) A), which is *trans* to the oxo-ligand, as it is observed in the $[MoO(acac)_2(PMe_3)]$ structure.[48]

Single crystals suitable for X-ray diffraction analysis of complex **8** were obtained from a saturated benzene-d_6 solution (a molecular view is given in Figure 8), and its structure in the solid state determined by X-ray diffraction. Table 4 contains selected bond lengths and angles for this derivative. Complex **8** crystallizes in the noncentrosymmetric monoclinic space group $P2_1$ as a single isomer, but the similar steric properties of the N^tBu and PMe_3 ligands (cone angles 126° and 131° as calculated from the X-ray data[50]) induce the presence of a crystallographic disorder in which the two groups exchange with each other in a nearly 1:1 ratio. A search in the CCDC database revealed that not many Mo^{IV} imido phosphine adducts are present in the literature, most of those featuring bulkier and more protecting =N—Ar groups. Moreover, the present derivative is the first reported example of a Mo^{IV} imido phosphine deriving from an OAT reaction. Scarcity of derivatives notwithstanding, two examples can be used for comparison, namely $[Mo(N^tBu)(PMe_3)(^tBu_3SiO)_2]$[51] and $[(\eta^5\text{-MeCp})Mo(N^tBu)(PMe_3)]^+$.[52] As in the oxo analogue, the Mo in complex **8** is octahedrally coordinated by two bidentate ketiminato ligands in a *trans* N,N configuration, leaving two

Table 5. Crystallographic Data and Structure Refinement Details for Complexes 2, 4, 5, and 8

	2	4	5•C_7H_8	8
empirical formula	$C_{26}H_{26}F_6MoN_2O_4$	$C_{30}H_{35}F_6MoN_3O_3$	$C_{32}H_{35}F_6MoN_2O_3P$	$C_{33}H_{44}F_6MoN_3O_3P$
M_r, g/mol	640.43	695.55	736.53	755.62
cryst description	shard, orange	block, yellow	block, green	block, purple
cryst syst	monoclinic	monoclinic	monoclinic	monoclinic
space group	$C2/c$	$P2_1/n$	$P2_1/c$	$P2_1$
a, Å	31.6359(19))	9.7563(5)	11.9011(8)	11.6011(6)
b, Å	12.8657(8)	25.5215(13)	20.1516(13)	12.9908(7)
c, Å	13.9803(8)	13.4956(7)	13.5855(10)	11.6276(6)
α, deg	90.00	90.00	90.00	90.00
β, deg	109.019(2)	110.223(2)	95.499(2)	101.049(2)
γ, deg	90.00	90.00	90.00	90.00
V, Å^3	5379.6(6)	3153.2(3)	3243.2(4)	1719.88(16)
Z	8	4	4	2
T, K	100(2)	100(2)	100(2)	100(2)
D_c, g/cm^3	1.581	1.465	1.508	1.459
μ(Mo Kα), mm^{-1}	0.564	0.486	0.524	0.494
F(000)	2592	1424	1504	780
reflns collected	82 813	123 069	96 367	48 378
unique reflns	7754	10253	15579	8845
reflns with $I \geq 2\sigma(I)$	6911	8501	13189	8620
R(int), $R(\sigma)$	0.0317, 0.0170	0.0331, 0.0381	0.0279, 0.0224	0.0287, 0.0196
no. params/restraints	358/0	425/0	440/3	510/18
final R1, wR2 ($I \geq 2\sigma$)	0.0251, 0.0637	0.0282, 0.0635	0.0324, 0.0722	0.0167, 0.0411
R indices (all data)	0.0306, 0.0685	0.0428, 0.0795	0.0436, 0.0805	0.0179, 0.0417
GOF on F^2	1.085	1.178	1.076	1.032
larg diff peak and hole, e/Å^3	0.562, −0.458	0.606, −0.685	1.125, −0.776	0.502, −0.370
CCDC deposition numbers	837153	837155	837154	837156

dx.doi.org/10.1021/ic201681u | Inorg. Chem. 2012, 51, 1440−1449

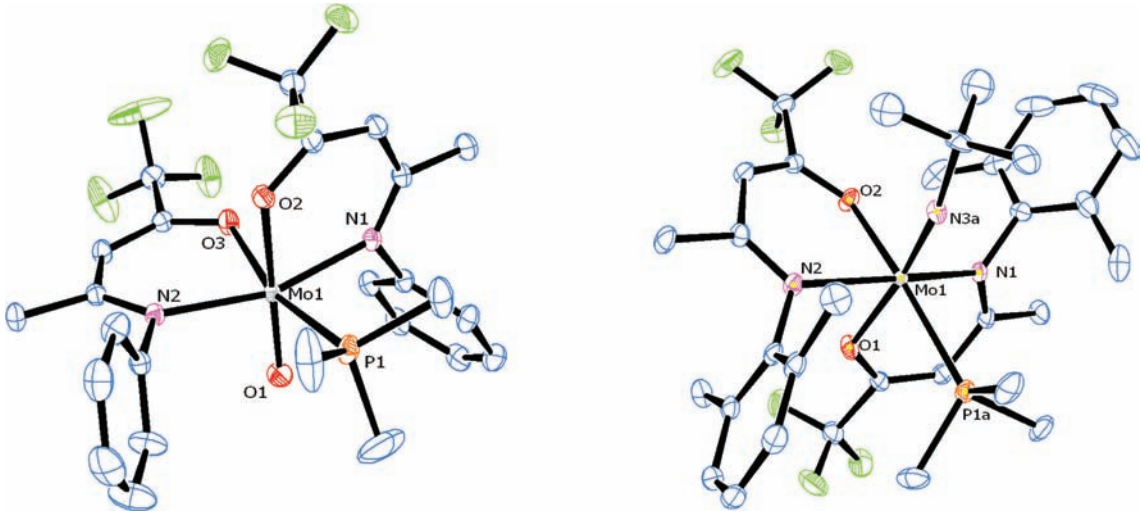

Figure 8. Thermal ellipsoid plot (30% probability level) of $[MoO(PMe_3)(L^H)_2]$ (**5**) (left) and $[Mo(N^tBu)(PMe_3)(L^{Me})_2]$ (**8**) (right). Hydrogen atoms and one molecule of cocrystallized toluene (for **5**) not shown for clarity.

residual sites for the N^tBu and PMe_3 groups arranged in a mutually *cis* disposition. The imido group is once more almost linear, although less so than in the Mo^{VI} analogue **4** (Mo−N−C angle 169.5(4)° for **8** vs 175.9(1) for **4**), as in the two reported examples, in contrast to aromatic imido complexes where the same group is almost invariably bent (av 160°). The Mo−P bond distance, at 2.541(1) Å, is sensibly longer than the two previously reported complexes (2.3202(8) and 2.443(5) Å, respectively) while a contraction is noticed in the Mo═N bond distance (1.703(3) vs 1.833(3) Å) indicating a greater degree of M→ N π-donation, in agreement with the (almost) linear coordination mode observed. No sensible variation is noted going from the oxo derivative **5** to **8**, suggesting little, if any at all, electronic contribution from the Mo═X (X = O, NR) moiety to the Mo—P fragment.

CONCLUSIONS

A new set of molybdenum dioxo and oxo-imido complexes, featuring the 2,6-disubstituted phenylimino-1,1,1-trifluoropentan-2-one ligand system, has been synthesized and characterized by spectroscopic means and by X-ray crystallography. The complexes were investigated in OAT reactions and the resulting reduced species isolated. The impact of the CF_3 electron withdrawing moiety was evaluated with kinetic measurements by UV−vis spectroscopy as well as by cyclic voltammetry. The insertion of such a moiety in the complex backbone increases the rate of the OAT reaction of a factor ranging between 14 and 92, depending on the heteroatom present on molybdenum and on the steric contraints imposed by the ketiminate ligand in contrast to a previous system.[46] The fluorinated group depletes the metal atom of electron density, thus making the bound oxo moiety much more susceptible to nucleophilic attack from the incoming oxygen atom acceptor. Moreover, the introduction of the electronegative group has allowed us to better differentiate electronic from steric effects and resolve the influences coming from the second doubly bonded atom. The dramatic increase in kinetic rate is, however, not reflected in a Mo═O bond length elongation in the solid state structures. Moreover, the first solid state characterization of a reduced imido phosphine Mo^{IV} complex deriving from an OAT reaction has been reported.

EXPERIMENTAL SECTION

General. All manipulations were carried out under dry argon using standard Schlenk line or glovebox techniques. All solvents were dried by a solvent purification system from Innovative Technology Inc. and flushed with argon prior to use. $[Mo(N^tBu)_2Cl_2(dme)]$ was prepared according to literature procedures.[53] All other chemicals mentioned were used as purchased from commercial sources. Samples for mass spectrometry were measured on an Agilent Technologies 5795C inert XL MSD spectrometer and all NMR spectra on a Bruker Avance 300 MHz spectrometer. Spectra were obtained at 25 °C unless otherwise noted. UV−vis spectra were recorded on a Varian Cary 50 spectrophotometer which was connected to a Hellma fiber optics all-quartz immersion probe.

UV−Vis Kinetic Experiments. In a typical experiment a stock solution was prepared, with 40 mg of the required complex dissolved in 20 mL of toluene (passed over alox). A 5-mL aliquot was then transferred in a 3-necked Schlenk flask and kept at the required temperature by means of a thermostat. Under a stream of argon gas the fiber optic probe was immersed in the solution and connected to the spectrophotometer. Via a syringe, the required amount of PMe_3 was added, and enough toluene was introduced so as to keep the total final volume of the solution the same throughout all the kinetic experiments. The measurement was started immediately after the addition.

Crystallography. Data were collected on a SMART APEX II diffractometer equipped with a CCD detector using graphite monochromated Mo Kα radiation (λ = 0.710 73 Å) and an Oxford cryostat (100(2) K); reduction, integration, and cell refinement were performed with SAINT.[54] The data sets were corrected for absorption and Lp effects with SADABS.[55] Structures were solved by direct methods (SHELX-97[56]), and refinement was carried on (full matrix least-squares on F^2) using the WINGX suite of programs.[57] All hydrogens atoms were added on calculated positions and refined isotropically. Graphical plots of the structures were made using ORTEP-3.[58] Crystallographic data (excluding structure factors) for the structures of compounds **2**, **4**, **5**, **8** reported in this paper and $[MoO\{N(2,6\text{-}Me_2C_6H_3)\}(L^{Me})_2]$ reported in the Supporting Information have been deposited with the Cambridge Crystallographic Data Center (CCDC 837153−837156 and 837220). Copies of the data can be obtained free of charge on application to the Director, CCDC, 12 Union Road, Cambridge CB2 1EZ, U.K. [fax (international) +44-1223/336-033; e-mail deposit@ccdc.cam.ac.uk].

General Procedure for the Synthesis of the ligands HL^R. The ligands were prepared according to a modification of the literature procedure[35] by condensation of 1,1,1-trifluoropentan-2,4-dione with the appropriate aromatic amine in benzene in the presence of catalytic

dx.doi.org/10.1021/ic201681u | Inorg. Chem. 2012, 51, 1440−1449

amounts of *p*-toluenesulfonic acid-monohydrate over molecular sieves. The mixture was refluxed until TLC showed no further changes, at which point it was filtered and the solvent was removed in vacuo, affording a red oil. The oil was taken up in a minimum amount of CH_2Cl_2, washed with diluted H_2SO_4, saturated $NaHCO_3$, and H_2O until neutrality; the organic layer was collected, dried over $MgSO_4$, and evaporated to dryness once more, prior to dissolution in petroleum ether, from which the product precipitated as colorless to yellow crystals upon cooling at −30 °C overnight.

HL^{Me}: Yield = 48.2%. ^{1}H NMR (300 MHz, C_6D_6): δ 1.05 (s, 3H, CH_3—C═N), 1.69 (s, 6H, CH_3—C_{Ar}), 5.43 (s, 1H, *γ-H*), 6.67−6.86 (m, 3H, H_{Ar}), 12.12 (br s, 1H, N*H*) ppm. ^{19}F NMR (282 MHz, C_6D_6): δ −76.15 (s, CF_3) ppm.

HL^{iPr}: Yield = 43.6%. ^{1}H NMR (300 MHz, C_6D_6): δ 0.89 (d, 6H, CH_3−CH−C_{Ar}, J_{H-H} = 6.8 Hz), 0.95 (d, 6H, CH_3−CH−C_{Ar}, J_{H-H} = 6.9 Hz), 1.21 (s, 3H, CH_3—C═N), 2.76 (sept, 2H, CH_3−*CH*−C_{Ar}, J_{H-H} = 6.8 Hz), 5.51 (s, 1H, *γ-H*), 6.90−7.10 (m, 3H, H_{Ar}), 12.61 (br s, 1H, N*H*) ppm. ^{19}F NMR (282 MHz, C_6D_6): δ −76.07 (s, CF_3) ppm. ^{13}C NMR (75 MHz, C_6D_6): δ 18.64 (s, CH_3—C═N), 22.10 (s, CH_3−CH−C_{Ar}), 23.89 (s, CH_3−CH−C_{Ar}), 28.55 (s, CH_3−*CH*−C_{Ar}), 89.48 (s, *γ-C*), 118.27 (q, CF_3, J_{C-F} = 288.77 Hz), 123.77 (s, C_{Ar}), 129.07 (s, C_{Ar}), 132.22 (s, C_{Ar}), 145.39 (s, C_{Ar}), 169.94 (s, *C*═N), 177.03 (q, *C*═N, J_{C-F} = 32,84 Hz) ppm.

HL^{H}: Yield = 70.5%. ^{1}H NMR (300 MHz, C_6D_6): δ 1.25 (s, 3H, CH_3—C═N), 5.35 (s, 1H, *γ-H*), 6.42−6.89 (m, 5H, H_{Ar}), 12.69 (br s, 1H, N*H*) ppm. ^{19}F NMR (282 MHz, C_6D_6): δ −76.25 (s, CF_3) ppm. ^{13}C NMR (75 MHz, C_6D_6): δ 19.09 (s, CH_3—C═N), 90.81 (s, *γ-C*), 118.05 (q, CF_3, J_{C-F} = 288.82 Hz), 124.63 (s, C_{Ar}), 126.55 (s, C_{Ar}), 128.93 (s, C_{Ar}), 136.88 (s, C_{Ar}), 167.04 (s, *C*═N), 176.55 (q, *C*═O, J_{C-F} = 32,82 Hz) ppm.

General Procedure for the Synthesis of $[MoO_2(L^R)_2]$. In a typical experiment, $[MoO_2Cl_2]$ (1 equiv) was suspended in toluene (10 mL), and a solution of the appropriate HL^R (2 equiv) and NEt_3 (2 equiv) in the same solvent (5 mL) was added dropwise. The reaction mixture immediately changed color to a deep red, whereby all of the suspended starting material dissolved. The mixture was left stirring for 12 h at room temperature and then filtered over Celite. The orange solution was then evaporated to dryness causing the formation of a yellow-orange solid, which was washed with 3 × 5 mL pentane and dried in vacuo, to afford $[MoO_2(L^R)_2]$.

$[MoO_2(L^H)_2]$ (1). The compound was prepared according to the general procedure, using 0.60 g of $[MoO_2Cl_2]$ (3.0 mmol) and 1.40 g of HL^H (6.1 mmol). Isolated yield after workup: 0.82 g (46%).

^{1}H NMR (300 MHz, C_6D_6, δ, ppm): 1.05 (s, 3H, *Me*), 6.43−7.12 (m, 10H, H_{Ar}), 5.68 (s, 1H, H_γ). ^{19}F NMR (282 MHz, C_6D_6, δ, ppm): −73.76 (s, CF_3). ^{13}C NMR (75 MHz, C_6D_6, δ, ppm): 24.2 (s, CH_3−CN), 100.56 (s, *γ-C*), 119.86 (q, CF_3, J_{C-F} = 282.2 Hz), 123.6, 124.0, 126.1, 129.0 (s, C_{Ar}), 152.49 (C_{ipso}), 164.25 (q, *C*═O, J_{C-F} = 35 Hz), 167.3 (s, CH_3-*C*N) ppm. EI-MS: 586.2 ($[M]^+$, 15%), 358.0 ($[M - L]^+$, 12%), 118.0 ($[Ar—N═C(CH_3)]^+$, 100%). Anal. Calcd for $C_{22}H_{18}F_6MoN_2O_4$: C, 45.22; H, 3.10; N, 4.79%. Found: C, 45.10; H, 3.35; N, 4.63%.

$[MoO_2(L^{Me})_2]$ (2). The compound was prepared according to the general procedure, using 0.15 g of $[MoO_2Cl_2]$ (0.75 mmol) and 0.40 g of HL^{Me} (1.6 mmol). Crystals suitable for X-ray diffraction analysis were grown from a cold solution (−30 °C) of the complex in MeCN. Isolated yield after workup: 0.39 g (81%). ^{1}H NMR (300 MHz, C_6D_6, δ, ppm): 1.06 (s, 3H, *Me*) 1.82 (s, 3H, Me_{ring}), 2.43 (s, 3H, Me_{ring}), 5.68 (s, 1H, H_γ), 6.73−6.85 (m, 6H, H_{Ar}). ^{19}F NMR (282 MHz, C_6D_6, δ, ppm): −73.81. ^{13}C NMR (75 MHz, C_6D_6, δ, ppm): 17.33 (*Me*), 17.99 (*Me*), 23.2 (*Me*), 99.2 (C_γ), 119.4 (q, J = 282.0, CF_3), 126.82, 128.52, 129.27, 130.14, 130.43 (C_{Ar}), 150.5 (ipso *C*), 163.2 (q, J = 34.2, *C*O), 176.18 (C═N). EI-MS: 642.2 ($[M]^+$, 15%), 386.0 ($[M - L]^+$, 7%), 146.0 ($[Ar—N═C(CH_3)]^+$, 100%). Anal. Calcd for $C_{26}H_{26}F_6MoN_2O_4$: C, 48.76; H, 4.09; N, 4.37%. Found: C, 48.59; H, 4.32; N, 4.25%.

$[MoO_2(L^{iPr})_2]$ (3). The compound was prepared according to the general procedure, using 0.14 g of $[MoO_2Cl_2]$ (0.7 mmol) and 0.44 g of HL^{iPr} (1.4 mmol). Isolated yield after workup: 0.16 g (28%). ^{1}H NMR (300 MHz, C_6D_6, δ, ppm): 0.72 (d, 6H, CH_3−CH−C_{Ar}, J_{H-H} = 6.8 Hz), 1.11 (d, 6H, CH_3−CH−C_{Ar}, J_{H-H} = 6.8 Hz), 1.22 (d, 6H, CH_3−CH−C_{Ar} overlapping with s, 6H, CH_3−C), 1.58 (d, 6H, CH_3−CH−C_{Ar}, J_{H-H} = 6.6 Hz), 2.67 (sept, 2H, CH_3−*CH*−C_{Ar}, J_{H-H} = 6.80 Hz), 3.59 (sept, 2H, CH_3−*CH*−C_{Ar}, J_{H-H} = 6.7 Hz), 5.69 (s, 2H, H_γ), 6.85−7.07 (m, 6H, H_{Ar}). ^{19}F NMR (282 MHz, C_6D_6, δ, ppm): −74.01 (s, CF_3). ^{13}C NMR (75 MHz, C_6D_6, δ, ppm): δ 24.13 (s, CH_3−CN), 24.61 (s, CH_3−CH), 24.89 (s, CH_3−CH), 25.16 (s, CH_3−CH), 25.2 (s, CH_3−CH), 28.03 (s, CH_3−CH), 28.27 (s, CH_3−*C*H), 99.03 (s, C_γ), 119.81 (q, CF_3, J_{C-F} = 282 Hz), 148.97 (C_{ipso}), 124.07, 124.4, 125.26 (s, C_{Ar}), 140.82 (s, *C*-iPr), 141.07 (s, *C*-iPr), 162.80 (q, *C*═O, J_{C-F} = 34.3 Hz), 177.15 (s, CH_3−*C*N). HR-MS Calcd for $C_{34}H_{42}F_6MoN_2O_4$: 748.2117. Found: 748.2167.

Synthesis of $[MoO(N^tBu)(L^{Me})_2]$ (4). $[MoO(N^tBu)Cl_2(dme)]$ (0.110 g, 0.32 mmol) was dissolved in 10 mL of toluene, and a solution of HL^{Me} (0.400 g, 0.64 mmol) and 0.25 mL of NEt_3 in 5 mL of toluene was added dropwise, with constant stirring. No evident color change was observed, and the reaction was left to stir overnight. The dark suspension (white solid visible) was then filtered over Celite to afford a dark orange solution. Evaporation of the toluene left a dark oily solid, which turned to a yellowish solid upon addition of 5 mL of pentane. The yellow powder was then filtered and dried in vacuo (0.150 g, 65%). Crystals suitable for X-ray diffraction were grown from a toluene/pentane solution of the complex at room temperature. ^{1}H NMR (300 MHz, C_6D_6, δ, ppm): 0.84 (s, 9H, *tBu*), 0.96 (s, 3H, *Me*), 1.22 (s, 3H, *Me*), 2.04 (s, 3H, *Me*), 2.27 (s, 3H, *Me*), 2.30 (s, 3H, *Me*), 2.42 (s, 3H, *Me*), 5.53 (s, 1H, H_γ), 5.63 (s, 1H, H_γ), 7.04−6.69 (m, 6H, aromatic). ^{19}F NMR (282 MHz, C_6D_6, δ, ppm): −73.24 (s, CF_3), −72.36 (s, CF_3). ^{13}C NMR (75 MHz, C_6D_6, δ, ppm): 18.2 (*Me*), 18.55 (*Me*), 19.0 (*Me*), 20.6 (*Me*), 23.2 (*Me*), 23.6 (*Me*), 28.7 (CMe_3), 73.8 (CMe_3), 97.7 (C_γ), 99.7 (C_γ), 119.9, 120.2 (overlapping q, J_{CF} = 287.6 and 284.0 Hz, CF_3), 126.6, 126.8, 128.95, 128.97, 129.4, 129.5 130.76, 130.9, 132.2, 133.6, 135.4, (C_{Ar}), 150.1 (C_{ipso}), 154.4 (C_{ipso}), 164.4, 164.7 (overlapping quartets J_{CF} = 33.2 and 32.7 Hz, *C*O), 175.2 (*C*═N), 175.5 (C═N). EI-MS: 697.5 ($[M]^+$, 12%), 626.3 ($[M - N^tBu]^+$, 12%), 146.2 ($[Ar—N═C(CH_3)]^+$, 100%). Anal. Calcd for $C_{30}H_{35}F_6MoN_3O_3$: C, 51.80; H, 5.07; N, 6.04%. Found: C, 51.44; H, 5.03; N, 6.41%.

General Procedure for the Synthesis of the Phosphine Mo^{IV} Adducts $[MoO(PMe_3)(L^R)_2]$. In a typical experiment $[MoO_2L_2]$ (1 equiv) was dissolved in 10 mL of toluene, and PMe_3 (0.1 mL) was added quickly via a syringe. The solution immediately turned deep green, and it was left stirring for 2 h at rt. The solvent was then removed in vacuo to afford a green powder, which was washed with 3 × 5 mL cold pentane and subjected to sublimation (0.05 mmHg, 70 °C) to remove residual $OPMe_3$. The products were isolated as green powders.

$[MoO(PMe_3)(L^H)_2]$ (5). The compound was prepared according to the general procedure, using 0.40 g of complex **1** (0.68 mmol). Isolated yield after workup: 0.35 g (79%). ^{1}H NMR (300 MHz, C_6D_6, δ, ppm): 0.55 (d, 9H, P*Me*$_3$, J_{HP} = 8.4 Hz), 1.27 (s, 3H, CH_3−C), 1.97 (s, 3H, CH_3−C), 5.49 (s, 1H, H_γ), 5.90 (s, 1H, H_γ), 6.77−7.06 (m, 10H, H_{Ar}). ^{19}F NMR (282 MHz, C_6D_6, δ, ppm): δ −73.33 (s, CF_3), −71.96 (s, CF_3). ^{31}P NMR (121 MHz, C_6D_6, δ, ppm): δ −1.28 (m, *P*Me$_3$, J_{PH} = 8.4 Hz) ppm. ^{13}C NMR (75 MHz, C_6D_6, δ, ppm): 15.45 (d, P*Me*$_3$, J_{C-P} = 22.2 Hz), 24.14 (s, CH_3−CN), 24.2 (s, CH_3−CN), 96.45 (C_γ), 97.21 (C_γ), 121.10, 122.99 (C_{Ar}), 123.75 (q, CF_3, J_{C-F} = 281.5 Hz), 124.17 (s, C_{Ar}), 124.45 (q, CF_3, J_{C-F} = 283,9 Hz), 124.97, 125.36, 125.71, 126.20, 128.95, 129.39, 129.8 (C_{Ar}), 152.7 (C_{ipso}), 156.5 (C_{ipso}), 160.75 (q, *C*═O, J_{C-F} = 31.5 Hz), 163.50 (q, *C*═O, J_{C-F} = 31.7 Hz), 165.53 (s, CH_3−*C*N), 171.8 (s, CH_3−*C*N). HR-MS Calcd for $C_{22}H_{18}F_6MoN_2O_3$ ($[M - PMe_3]^+$): 564.0290. Found: 564.0321.

$[MoO(PMe_3)(L^{Me})_2]$ (6). The compound was prepared according to the general procedure, using 0.27 g of complex **2** (0.42 mmol). Isolated yield after workup: 0.24 g (81%). ^{1}H NMR (300 MHz, C_6D_6, δ, ppm): 0.58 (d, 9H, J_{PH} = 7.84 Hz, P*Me*$_3$), 1.19 (s, 3H, *Me*), 1.84 (s, 3H, *Me*), 2.20 (s, 3H, *Me*), 2.27 (s, 3H, *Me*), 2.25 (s, 3H, *Me*), 2.31 (s, 3H, *Me*), 5.48 (s, 1H, H_γ), 5.82 (s, 1H, H_γ), 6.82 (m, 6H, aromatic). ^{19}F NMR (282 MHz, C_6D_6, δ, ppm): −72.44 (s, CF_3), −71.27 (s, CF_3). ^{31}P NMR (121 MHz, C_6D_6, δ, ppm): −7.1. ^{13}C NMR (75 MHz,

dx.doi.org/10.1021/ic201681u | *Inorg. Chem.* 2012, 51, 1440−1449

C_6D_6, δ, ppm): 16.30 (d, J_{PC} = 20.9 Hz, P*Me*$_3$), 18.13 (*Me*), 18.24 (*Me*), 19.74 (*Me*), 19.77 (*Me*), 21.05 (*Me*), 23.57 (*Me*), 24.19 (*Me*), 96.50 (C_γ), 98.74 (C_γ), 119.4 (q, J = 282.0 Hz, CF_3), 123.1 (q, J = 280 Hz, CF_3), 125.57, 126.19, 128.86, 129.35, 129.60, 130.73, 132.47, 133.33 (C_{Ar}), 150.6 (C_{ipso}), 154.64 (C_{ipso}), 160.2 (q, J = 34.2, *CO*), 164.3 (q, J = 34.0 Hz), 172.60 (C═N), 173.65 (C═N). HR-MS Calcd for $C_{26}H_{26}F_6MoN_2O_3$ ([M − PMe_3]$^+$): 620.0916. Found: 620.0925.

[MoO(PMe$_3$)(L^{iPr})$_2$] (7). The compound was prepared according to the general procedure, using 0.42 g of complex **3** (0.55 mmol). Isolated yield after workup: 0.40 g (89%). ^{1}H NMR (300 MHz, C_6D_6, δ, ppm): 0.55 (d, 9H, P*Me*$_3$, J_{HP} = 8.1 Hz), 0.92 (d, 3H, J_{HH} = 6.2 Hz, *Me*), 0.96 (d, 3H, J_{HH} = 6.2 Hz, *Me*), 1.01 (d, 3H, J_{HH} = 6.2 Hz, *Me*), 1.12 (d, 3H, J_{HH} = 6.2 Hz, Me), 1.14 (d, 3H, J_{HH} = 6.2 Hz, *Me*), 1.34 (d, 3H, J_{HH} = 6.2 Hz, *Me*), 1.46 (d, 3H, J_{HH} = 6.2 Hz, *Me*), 1.49 (d, 3H, J_{HH} = 6.2 Hz, *Me*), 1.58 (s, 3 H, *Me*), 2.01 (s, 3 H, *Me*), 3.14 (sept, 1H, J_{HH} = 6.2 Hz, *CH*), 3.26 (sept, 1H, J_{HH} = 6.2 Hz, *CH*), 3.36 (sept, 1H, J_{HH} = 6.2 Hz, *CH*), 3.70 (sept, 1H, J_{HH} = 6.2 Hz, *CH*), 5.77 (s, 1H, H_γ), 5.92 (s, 1H, H_γ), 7.06 (m, 6 H, aromatic). ^{19}F NMR (282 MHz, C_6D_6, δ, ppm): −73.34 (s, CF_3), −71.92 (s, CF_3). ^{31}P NMR (121 MHz, C_6D_6, δ, ppm): −1.24. ^{13}C NMR (75 MHz, C_6D_6, δ, ppm): 16.16 (d, J_{P-C} = 22 Hz, P*Me*$_3$), 22.09 (Me_{iPr}), 23.25 (Me_{iPr}), 25.95 (Me_{iPr}), 23.55 (Me_{iPr}), 22.52 (Me_{iPr}), 25.52 (Me_{iPr}), 25.62 (Me_{iPr}), 23.09 (Me_{iPr}), 20.04 (*Me*), 28.52 (*Me*), 26.86 (CH), 27.07 (CH), 28.19 (CH), 29.67 (CH), 98.06, 98.15 (C_γ). HR-MS Calcd for $C_{34}H_{42}F_6MoN_2O_3$ ([M − PMe_3]$^+$): 732.2168. Found: 732.2167.

Synthesis of [Mo(N^{t}Bu)(PMe$_3$)(L^{Me})$_2$] (8). [MoO(N^{t}Bu)(L^{Me})$_2$] (**4**) (0.25 g, 0.36 mmol) was dissolved in 10 mL of toluene, and PMe_3 (0.1 mL, 2.6 equiv) was added quickly via a syringe. The solution immediately turned deep purple, and it was left stirring for 6 h at room temperature. The solvent was then removed in vacuo to afford a violet powder, which was washed with 3 × 5 mL cold pentane and subjected to sublimation (0.05 mmHg, 70 °C) to remove residual $OPMe_3$ (yield 0.22 g, 82%).

^{1}H NMR (300 MHz, C_6D_6, δ, ppm): 0.51 (d, 9H, J_{PH} = 7.20 Hz, P*Me*$_3$), 1.08 (s, 9H, ^{t}*Bu*), 1.8 (s, 3H, *Me*), 1.24 (s, 3H, *Me*), 2.09 (s, 3H, *Me*), 2.15 (s, 3H, *Me*), 2.24 (s, 3H, *Me*), 2.44 (s, 3H, *Me*), 5.36 (s, 1H, H_γ), 5.96 (s, 1H, H_γ), 6.73−7.03 (m, 6H, aromatic). ^{19}F NMR (282 MHz, C_6D_6, δ, ppm): −72.23 (s, CF_3), −69.97 (s, CF_3). ^{31}P (121 MHz, C_6D_6, δ, ppm): 2.82 (P*Me*$_3$). ^{13}C NMR (75 MHz, C_6D_6, δ, ppm): 17.60 (d, P*Me*$_3$, J_{CP} = 6.7 Hz), 17.29 (*Me*), 18.57 (*Me*), 22.14 (*Me*), 23.27 (*Me*), 23.42 (*Me*), 29.62 (C*Me*$_3$), 23.94 (*Me*), 72.25 (C*Me*$_3$), 96.96 (C_γ), 97.97 (C_γ), 116.03 (CF_3, q, J_{CF} = 282.3 Hz), 120.12 (CF_3, q, J_{CF} = 284.7 Hz), 125.32, 125.72, 128.68, 128.71, 129.98, 130.05, 133.88, 134.47, 135.46 (C_γ), 154.05 (C_{ipso}), 154.20 (C_{ipso}), 158.40 (q, $COCF_3$, J_{CF} = 31.24 Hz), 164.27 (q, $COCF_3$, J_{CF} = 30.47 Hz), 167.94 (C═N), 170.60 (C═N). HR-MS Calcd for $C_{30}H_{35}F_6MoN_3O_2$ ([M − PMe_3]$^+$): 675.1702. Found: 675.1731.

■ ASSOCIATED CONTENT

Supporting Information

CIF data. Additional figures and table. This material is available free of charge via the Internet at http://pubs.acs.org.

■ AUTHOR INFORMATION

Corresponding Author

*E-mail: nadia.moesch@uni-graz.at.

■ ACKNOWLEDGMENTS

Financial support by the Austrian Science Foundation FWF P19309-N19 is gratefully acknowledged.

■ REFERENCES

(1) Brégeault, J.-M. *Dalton Trans.* **2003**, 3289−3302.
(2) Brondino, C. D.; Rivas, M. G.; Romão, M. J.; Moura, J. J. G.; Moura, I. *Acc. Chem. Res.* **2006**, *39*, 788−796.
(3) Hille, R. *Chem. Rev.* **1996**, *96*, 2757−2816.
(4) Romão, M. J. *Dalton Trans.* **2009**, 4053−4068.
(5) Enemark, J. H.; Cooney, J. J. A.; Wang, J.-J.; Holm, R. H. *Chem. Rev.* **2004**, *104*, 1175−1200.
(6) Johnson, M. K.; Rees, D. C.; Adams, M. W. W. *Chem. Rev.* **1996**, *96*, 2817−2840.
(7) Bray, R. C.; Adams, B.; Smith, A. T.; Bennett, B.; Bailey, S. *Biochemistry* **2000**, *39*, 11258−11269.
(8) Li, H.-K.; Temple, C.; Rajagopalan, K. V.; Schindelin, H. *J. Am. Chem. Soc.* **2000**, *122*, 7673−7680.
(9) Schrader, N.; Fischer, K.; Theis, K.; Mendel, R.; Schwarz, G.; Kisker, C. *Structure* **2003**, *11*, 1251−1263.
(10) Moura, J. J. G.; Brondino, C. D.; Trincao, J.; Romao, M. J. *JBIC, J. Biol. Inorg. Chem.* **2004**, *9*, 791−799.
(11) Schulzke, C. *Eur. J. Inorg. Chem.* **2011**, 1189−1199.
(12) Sugimoto, H.; Tsukube, H. *Chem. Soc. Rev.* **2008**, *37*, 2609−2619.
(13) Mösch-Zanetti, N. C.; Wurm, D.; Volpe, M.; Lyashenko, G.; Harum, B.; Belaj, F.; Baumgartner, J. *Inorg. Chem.* **2010**, *49*, 8914−8921.
(14) Doonan, C. J.; Millar, A. J.; Nielsen, D. J.; Young, C. G. *Inorg. Chem.* **2005**, *44*, 4506−4514.
(15) Doonan, C. J.; Nielsen, D. J.; Smith, P. D.; White, J. M.; George, G. N.; Young, C. G. *J. Am. Chem. Soc.* **2006**, *128*, 305−316.
(16) Sugimoto, H.; Tatemoto, S.; Suyama, K.; Miyake, H.; Mtei, R. P.; Itoh, S.; Kirk, M. L. *Inorg. Chem.* **2010**, *49*, 5368−5370.
(17) Mondal, J. U.; Almaraz, E.; Bhat, N. G. *Inorg. Chem. Commun.* **2004**, *7*, 1195−1197.
(18) Nemykin, V. N.; Davie, S. R.; Mondal, S.; Rubie, N.; Kirk, M. L.; Somogyi, A.; Basu, P. *J. Am. Chem. Soc.* **2002**, *124*, 756−757.
(19) Sinclair, L. *Inorg. Chim. Acta* **1998**, *278*, 1−5.
(20) Murdzek, J. S.; Schrock, R. R. *Organometallics* **1987**, *6*, 1373−1374.
(21) Belgacem, J.; Kress, J.; Osborn, J. A. *J. Am. Chem. Soc.* **1992**, *114*, 1501−1502.
(22) Takacs, J.; Cavell, R. G. *Inorg. Chem.* **1994**, *33*, 2635−2638.
(23) Vaughan, W. *J. Organomet. Chem.* **1995**, *485*, 37−43.
(24) Cantrell, G. K.; Geib, S. J.; Meyer, T. Y. *Organometallics* **2000**, *19*, 3562−3568.
(25) Gibson, V. C.; Graham, A. J.; Jolly, M.; Mitchell, J. P. *Dalton Trans.* **2003**, 4457−4465.
(26) Ramnauth, R.; Al-Juaid, S.; Motevalli, M.; Parkin, B. C.; Sullivan, A. C. *Inorg. Chem.* **2004**, *43*, 4072−4079.
(27) Radius, U.; Wahl, G.; Sundermeyer, J. *Z. Anorg. Allg. Chem.* **2004**, *630*, 848−857.
(28) Merkoulov, A.; Harms, K.; Sundermeyer, J. *Eur. J. Inorg. Chem.* **2005**, 4902−4906.
(29) Cross, W. B.; Anderson, J. C.; Wilson, C.; Blake, A. J. *Inorg. Chem.* **2006**, *45*, 4556−4561.
(30) Cross, W. B.; Anderson, J. C.; Wilson, C. S. *Dalton Trans.* **2009**, 1201−1205.
(31) Thrasher, J. S.; Strauss, S. H. *Inorganic fluorine chemistry: toward the 21st century* (Washington, DC, 1994).
(32) Li, X.-F.; Dai, K.; Ye, W.-P.; Pan, L.; Li, Y.-S. *Organometallics* **2004**, *23*, 1223−1230.
(33) Yu, S.-M.; Mecking, S. *J. Am. Chem. Soc.* **2008**, *130*, 13204−13205.
(34) Long, Y.-Y.; Ye, W.-P.; Tao, P.; Li, Y.-S. *Dalton Trans.* **2011**, *40*, 1610−1618.
(35) Yu, S.-M.; Tritschler, U.; Göttker-Schnetmann, I.; Mecking, S. *Dalton Trans.* **2010**, *39*, 4612−4618.
(36) Tang, L.-M.; Wu, J.-Q.; Duan, Y.-Q.; Pan, L.; Li, Y.-G.; Li, Y.-S. *J. Polym. Sci., Part A: Polym. Chem.* **2008**, *46*, 2038−2048.
(37) Xing, Y.; He, X.; Chen, Y.; Nie, H.; Wu, Q. *Polym. Bull.* **2011**, *66*, 1149−1161.
(38) Zhang, L.; Brookhart, M.; White, P. S. *Organometallics* **2006**, *25*, 1868−1874.
(39) Huang, Y.-B.; Jin, G.-X. *Dalton Trans.* **2009**, 767−769.
(40) Modi, C. K.; Thaker, B. T. *J. Therm. Anal. Calorim.* **2008**, *94*, 567−577.
(41) Sloop, J. C. *J. Phys. Org. Chem.* **2009**, *22*, 110−117.

(42) Lyashenko, G.; Saischek, G.; Judmaier, M. E.; Volpe, M.; Baumgartner, J.; Belaj, F.; Jancik, V.; Herbst-Irmer, R.; Mösch-Zanetti, N. C. *Dalton Trans.* **2009**, 5655–5665.
(43) Cross, W. B.; Anderson, J. C.; Wilson, C.; Blake, A. J. *Inorg. Chem.* **2006**, *45*, 4556–4561.
(44) Hänninen, M. M.; Sillanpää, R.; Kivelä, H.; Lehtonen, A. *Dalton Trans.* **2011**, *40*, 2868–2874.
(45) Rufanov, K. A.; Kipke, J.; Sundermeyer, J. *Dalton Trans.* **2011**, *40*, 1990–1997.
(46) Basu, P.; Nemykin, V. N.; Sengar, R. S. *Inorg. Chem.* **2009**, *48*, 6303–6313.
(47) Stiefel, E. I. *Progress in Inorganic Chemistry*; John Wiley & Sons, Inc.: Hoboken, NJ, 1977; Vol. *22*, p 1.
(48) Rogers, R. *J. Organomet. Chem.* **1984**, *277*, 403–415.
(49) Atwood, J. L.; Darensbourg, D. J. *Inorg. Chem.* **1977**, *16*, 2314–2317.
(50) Müller, T.; Mingos, D.; Michael, P. *Transition Met. Chem.* **1995**, *20*, 533–539.
(51) Rosenfeld, D. C.; Wolczanski, P. T.; Barakat, K. A.; Buda, C.; Cundari, T. R.; Schroeder, F. C.; Lobkovsky, E. B. *Inorg. Chem.* **2007**, *46*, 9715–9735.
(52) Green, M. L. H.; Konidaris, P. C.; Michaelidou, D. M.; Mountford, P. *J. Chem. Soc., Dalton Trans.* **1995**, 155–162.
(53) Fox, H. H.; Yap, K. B.; Robbins, J.; Cai, S.; Schrock, R. R. *Inorg. Chem.* **1992**, *31*, 2287–2289.
(54) *SAINTPLUS: Software Reference Manual, Version 6.4*; Bruker AXS: Madison, WI, 1997.
(55) *SADABS, Version 2.1*; Bruker AXS: Madison, WI, 1998.
(56) Sheldrick, G. M. *Acta Crystallogr., Sect. A* **2008**, *64*, 112–122.
(57) Farrugia, L. J. *J. Appl. Crystallogr.* **1999**, *32*, 837–838.
(58) Farrugia, L. J. *J. Appl. Crystallogr.* **1997**, *30*, 565.